Langmuir
Article
pubs.acs.org/Langmuir
© 2011 American Chemical Society

# A Convenient Route to High Area, Nanoparticulate $TiO_2$ Photoelectrodes Suitable for High-Efficiency Energy Conversion in Dye-Sensitized Solar Cells

Nak Cheon Jeong, Omar K. Farha, and Joseph T. Hupp*

*Department of Chemistry and Argon-Northwestern Solar Energy Research Center (ANSER), Northwestern University, 2145 Sheridan Road, Evanston, Illinois 60208, United States*

*Received October 26, 2010. Revised Manuscript Received December 16, 2010*

Ethanol-soluble amphiphilic $TiO_2$ nanoparticles (NPs) of average diameter ~9 nm were synthesized, and an α-terpineol-based $TiO_2$ paste was readily prepared from them in comparatively few steps. When used for fabrication of photoelectrodes for dye-sensitized solar cells (DSSCs), the paste yielded highly transparent films and possessing greater-than-typical, thickness-normalized surface areas. These film properties enabled the corresponding DSSCs to produce high photocurrent densities (17.7 mA $cm^{-2}$) and a comparatively high overall light-to-electrical energy conversion efficiency (9.6%) when deployed with the well-known ruthenium-based molecular dye, N719. These efficiencies are about ~1.4 times greater than those obtained from DSSCs containing photoelectrodes derived from a standard commercial source of $TiO_2$ paste.

## Introduction

Dye-sensitized solar cells (DSSCs) have received considerable scientific and commercial attention on account of their (as yet unrealized) potential for achieving solar-to-electrical energy conversion at a cost equal to, or less than, that attainable with silicon-based photovoltaics.[1−7] Major improvements will likely require new redox shuttles (capable of supporting higher photovoltages) and new far-red-absorbing dyes (capable of increasing red and far-red light-harvesting efficiencies and thereby improving photocurrents). Unfortunately, attempts to evaluate the absolute performance of candidate dyes and shuttles are often complicated by issues relating to the underlying photoelectrode.

In the most highly efficient DSSCs, the photoanode includes a high-area $TiO_2$ film consisting of a mesoporous network of $TiO_2$ nanoparticles (NPs). Since the particle network serves as both a high-area scaffold for dye molecules and a conduit for delivering injected electrons to an underlying current collector, typically fluorine-doped tin oxide (FTO),[1,2] the size of particles and their degree of electrical interconnection can influence greatly the performance of a DSSC. Electrodes fabricated from readily available, commercial $TiO_2$ NP paste, or from easily synthesized $TiO_2$ NP paste, tend to yield mediocre cells, even when combined with components comprising champion cells (i.e., components of DSSCs of 11+% energy conversion efficiency, $\eta$).[8] Nevertheless, these approaches are often employed since the preparation of photoanodes capable of yielding high-performance cells is a lengthy and tedious process, entailing a large number of intermediate steps (see Scheme 1A). Here we report a simple and convenient method for constructing high-area $TiO_2$ NP electrodes. We find that these electrodes yield cells that deliver efficiencies that reasonably closely approach those of much-more-difficult-to-make champion DSSCs.[8,9]

## Limitations of Standard Approaches

Most DSSC-relevant $TiO_2$ pastes have been prepared either in water[10,11] or α-terpineol.[8,9,12,13] Since $TiO_2$ NPs are usually synthesized in aqueous solution via a hydrothermal reaction, they are initially well dispersed. Hence, water-based $TiO_2$ pastes are typically relatively easy to prepare. Water, however, induces agglomeration of $TiO_2$ NPs during the drying of the paste; this leads to diminished transparency for the $TiO_2$ films, and thus negatively affects the performance of the cells. In contrast, $TiO_2$ films fabricated with α-terpineol-based $TiO_2$ pastes are highly transparent and show good long-term stability. The process to make the pastes entails the exchange of water for ethanol and, subsequently, ethanol for α-terpineol. Because their surfaces are hydrophilic, $TiO_2$ NPs are immediately agglomerated by addition of ethanol, a solvent that is at least partially hydrophobic − especially in comparison to water (Scheme 2). Unfortunately, once NPs have agglomerated, they are difficult to redisperse in ethanol. Consequently, consistent preparation of high-quality α-terpineol-based $TiO_2$ pastes[9] can be challenging. These difficulties are compounded when syntheses of pastes comprising smaller NPs (diameter ($d$) < 10 nm) are attempted, as smaller

*To whom correspondence should be addressed. E-mail: j-hupp@northwestern.edu.

(1) Oregan, B.; Gratzel, M. *Nature* **1991**, *353*, 737–740.
(2) Hagfeldt, A.; Gratzel, M. *Acc. Chem. Res.* **2000**, *33*, 269–277.
(3) Gratzel, M. *Nature* **2001**, *414*, 338–344.
(4) Hamann, T. W.; Martinson, A. B. E.; Elam, J. W.; Pellin, M. J.; Hupp, J. T. *Adv. Mater.* **2008**, *20*, 1560–1564.
(5) Snaith, H. J. *Adv. Funct. Mater.* **2010**, *20*, 13–19.
(6) Meyer, G. J. *ACS Nano* **2010**, *4*, 4337–4343.
(7) Kalyanasundaram, K., *Dye-Sensitized Solar Cell*, 1st ed.; EPFL Press: Lausanne, Switzerland, 2010.
(8) Nazeeruddin, M. K.; De Angelis, F.; Fantacci, S.; Selloni, A.; Viscardi, G.; Liska, P.; Ito, S.; Bessho, T.; Gratzel, M. *J. Am. Chem. Soc.* **2005**, *127*, 16835–16847.
(9) Ito, S.; Chen, P.; Comte, P.; Nazeeruddin, M. K.; Liska, P.; Pechy, P.; Gratzel, M. *Prog. Photovoltaics* **2007**, *15*, 603–612.
(10) Zhang, D. S.; Ito, S.; Wada, Y. J.; Kitamura, T.; Yanagida, S. *Chem. Lett.* **2001**, 1042–1043.
(11) Tae, E. L.; Lee, S. H.; Lee, J. K.; Yoo, S. S.; Kang, E. J.; Yoon, K. B. *J. Phys. Chem. B* **2005**, *109*, 22513–22522.
(12) Ito, S.; Nazeeruddin, M. K.; Liska, P.; Comte, P.; Charvet, R.; Pechy, P.; Jirousek, M.; Kay, A.; Zakeeruddin, S. M.; Gratzel, M. *Prog. Photovoltaics* **2006**, *14*, 589–601.
(13) Lee, G. W.; Bang, S. Y.; Lee, C.; Kim, W. M.; Kim, D.; Kim, K.; Park, N. G. *Curr. Appl. Phys.* **2009**, *9*, 900–906.

**Scheme 1. Flow Charts of Procedures for Preparation of One Type of $TiO_2$ Paste[9] (Top) and TBA-$TiO_2$ Paste (Bottom)**

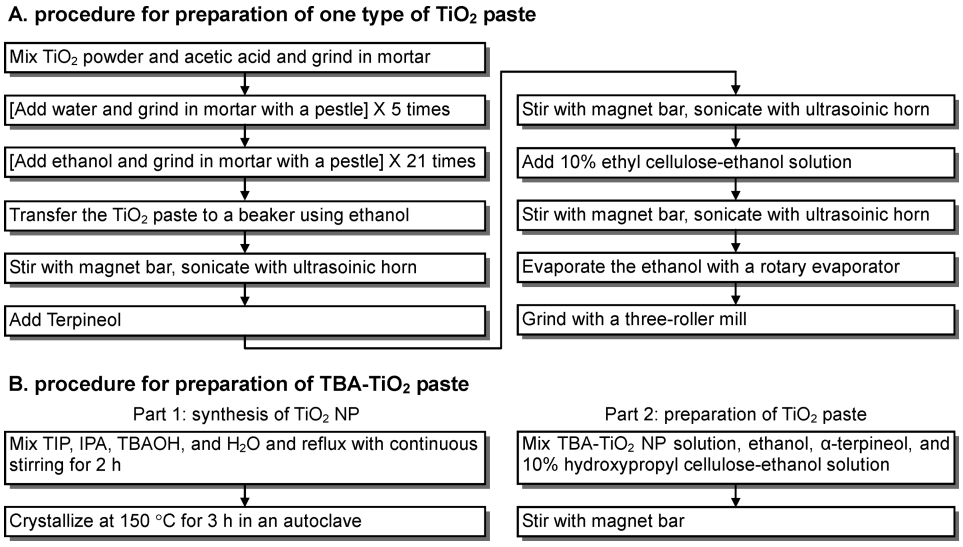


**Scheme 2. Qualitative Representations of Surfaces of Typical $TiO_2$ NPs (Left), TMA-$TiO_2$ NPs (Middle), and TBA-$TiO_2$ NPs (Right).**[a]

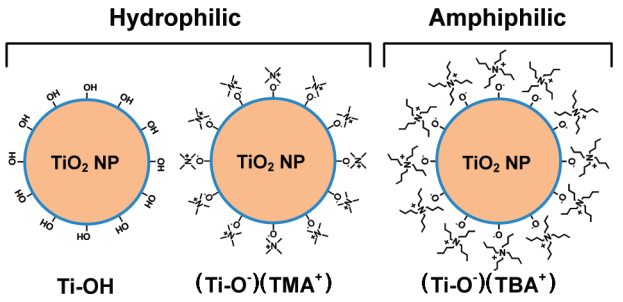


[a] While typical $TiO_2$ and TMA-$TiO_2$ NPs are hydrophilic, TBA-$TiO_2$ NPs are amphiphilic.

particles more readily agglomerate in nonaqueous solvents than do larger ones. Thus, published syntheses typically include steps where aggregated $TiO_2$ NPs are fractured using a mortar and pestle and then agitated to achieve some degree of redispersion in ethanol, followed by exchange with α-terpineol. In our experience, the extent of success with the redispersion steps is highly variable, such that the quality of the resulting paste is both difficult to predict and difficult to control.

## An Alternative Approach to $TiO_2$ NP-Paste Synthesis

Due to the presence of surface hydroxyl groups, NPs of $TiO_2$ typically are hydrophilic (Scheme 2). Thus, they are well dispersed in water, but not in hydrophobic or amphiphilic solvents. We reasoned that particles might be rendered hydrophobic—and their solubility therefore changed—by coating their surfaces with tetraalkylammonium ions. The preparation of coated particles is outlined in Scheme 1B and detailed in the Supporting Information (SI). Briefly, however, titanium(IV) isopropoxide (TIP) in isopropanol was added to an aqueous solution that had been made basic via addition of tetrabutylammonium hydroxide (TBAOH). Hydrolysis of TIP under these conditions (i.e., at a pH well above the pH-of-zero-charge for $TiO_2$) is expected to yield colloidal particles having substantial negative charge. The excess charge can be partially compensated via adsorption of $TBA^+$.[14] Colloidal particle suspensions were also prepared by

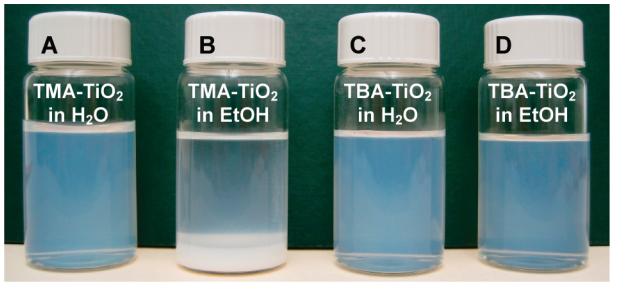


**Figure 1.** Photographs of (A) TMA-$TiO_2$ NPs dispersed in water, (B) sedimented TMA-$TiO_2$ agglomerates in EtOH, (C) TBA-$TiO_2$ NPs dispersed in water, and (D) TBA-$TiO_2$ NPs dispersed in EtOH.

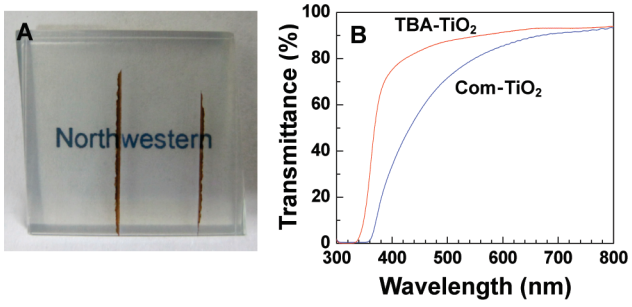


**Figure 2.** (A) Photograph of TBA-$TiO_2$ film, and (B) transmittance spectra of TBA-$TiO_2$ film (red curve) and Com-$TiO_2$ film (blue curve).

using tetramethylammonium hydroxide (TMAOH) in place of TBAOH. Powder X-ray diffraction (XRD) patterns of the synthesized TMA- and TBA-$TiO_2$ NPs (as well as the commercial sample) indicate that they are crystalline anatase (see SI).

Transmission electron microscopy (TEM) showed that the TMA-$TiO_2$ and TBA-$TiO_2$ NPs range in size (diameter) from ~5 nm to ~20 nm (see SI). Average sizes of NPs were calculated from the width of an X-ray diffraction peak characteristic of the (200) plane ($2\theta$ = 48.02°) by using the Debye−Scherrer method.[15,16] The average diameters of both the TBA- and TMA-capped particles are ca. 9 nm (see SI). The TMA-$TiO_2$ NPs were observed

(14) Kim, Y. J.; Chai, S. Y.; Lee, W. I. *Langmuir* **2007**, *23*, 9567–9571.

(15) Scherrer, P. *Göttinger Nachr.* **1918**, *26*, 98–100.
(16) Patterson, A. L. *Phys. Rev.* **1939**, *56*, 978.

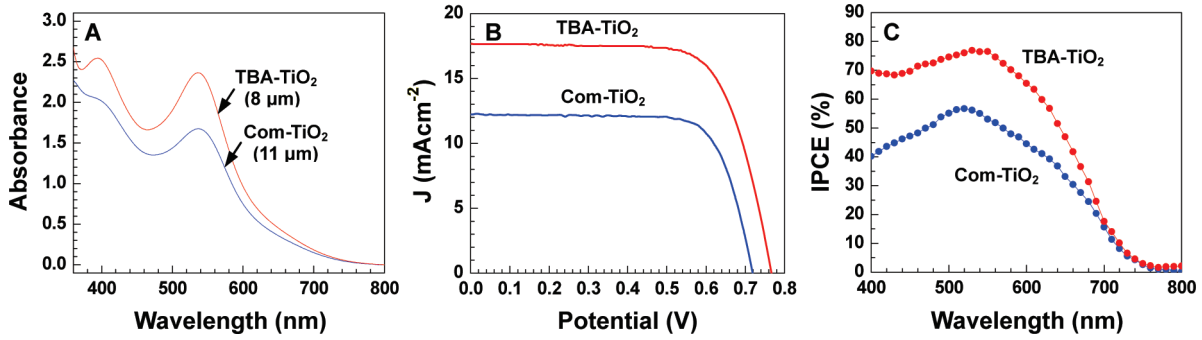


**Figure 3.** (A) UV−vis absorption spectra of N719-coated, 8 $\mu$m-thick TBA-$TiO_2$ film (red), and 11 $\mu$m-tick Com-$TiO_2$ film (blue). Extinction spectra for dye-free TBA-$TiO_2$ and Com-$TiO_2$ films were subtracted from spectra shown. (B) Corresponding $J-V$ curves for DSSCs assembled from the films. (C) Corresponding IPCE curves for DSSCs assembled from the films. Films examined in panel A did not include light-scattering layers (400-nm particle layers), while those examined in panels B and C did include such layers.

to disperse well in water, but immediately agglomerated and then precipitated when placed in ethanol (Scheme 2 and Figure 1A,B). The TBA-$TiO_2$ NPs, however, were observed to disperse well in both solvents (see panels C and D of Figure 1).

## Thin-Film Fabrication

The observed amphiphilicity of the TBA-$TiO_2$ NPs was anticipated to facilitate the preparation of high-quality pastes. Indeed, an α-terpineol-based paste proved straightforward to prepare by mixing TBA-$TiO_2$ NPs with ethanol, α-terpineol, and hydroxypropyl cellulose (see SI for further details). $TiO_2$ films were prepared from the paste by using the doctor-blade method (see SI). For comparison, we also prepared films from commercial $TiO_2$ paste (Com-$TiO_2$; product "DSL 18NR-T" from Dyesol) containing NPs of average diameter 17 nm (see SI). The thicknesses of TBA-$TiO_2$- and Com-$TiO_2$-derived films were ~8 $\mu$m and ~11 $\mu$m, respectively (see SI). As shown in Figure 2, TBA-$TiO_2$ films exhibit excellent transparency, with transmittance superior to that of Com-$TiO_2$-derived films in the 400−700 nm spectral region. We attribute the enhanced transparency for the TBA-$TiO_2$-derived films to less light scattering. In the Rayleigh scattering regime,

$$I = I_0\left(\frac{d}{2}\right)^6 \frac{1+\cos^2\theta}{2R^2}\left(\frac{2\pi}{\lambda}\right)^4\left(\frac{n^2-1}{n^2+2}\right)^2 \quad (1)$$

where $I$ is the intensity of scattered light, $I_0$ is the intensity of incident light, $d$ is the particle diameter, $\theta$ is the scattering angle, $R$ is the distance between observer and particle, $\lambda$ is the wavelength of incident light, and $n$ is the refractive index of the particle. Note that the amount of scattering scales as $d$ to the sixth power. Since TBA-$TiO_2$ NPs are roughly 2 times smaller (in diameter) than commercial $TiO_2$ NPs, the amount of scattered light from TBA-$TiO_2$ NPs should be $(1/2)^6$ times less than that from Com-$TiO_2$ NPs. Thus, we attribute the high transparency of TBA-$TiO_2$-derived films to the small size of the NPs.

The pore-size distributions of the two kinds of films were determined by collecting $N_2$ isotherms and then applying the Barrett−Joyner−Halenda (BJH) analysis (SI-7).[17] Consistent with the difference in component particle size, the average pore-size within TBA-$TiO_2$ films ($D_{max}$ = ~14 nm) was found to be considerably smaller than within Com-$TiO_2$ films ($D_{max}$ = ~30 nm). Furthermore, the pore-size distribution for TBA-$TiO_2$-derived films was found to be sharper than for Com-$TiO_2$-derived films. The isotherm-derived, BJH desorption pore volume per gram ($V_{P/W}$) and surface area per gram ($A_{/W}$) were used to calculate the BJH surface area per unit volume ($A_{/V}$; see SI). The values of $A_{/V}$ for TBA-$TiO_2$- and Com-$TiO_2$-derived films, respectively, were found to be 195 $m^2$/mL and 110 $m^2$/mL, yielding a ratio of 1.77. The Brunauer−Emmett−Teller (BET) surface areas are 84 $m^2g^{-1}$ for TBA-$TiO_2$ and 64 $m^2g^{-1}$ for Com-$TiO_2$. The densities of the films were obtained by dividing values for $A_V$ ($m^2$/mL) by the corresponding BET surface areas ($m^2$ $g^{-1}$). The density of TBA-$TiO_2$-derived films (2.31 g $mL^{-1}$) was found to be considerably higher than that of Com-$TiO_2$-derived films (1.72 g $mL^{-1}$), indicating that the NPs comprising the former are more closely packed and leave a smaller fraction of void volume.

## Evaluation in Solar Cells

The archetypal DSSC dye, N719 (a broadly absorbing, ruthenium coordination complex) was loaded onto film electrodes of both TBA-$TiO_2$ and Com-$TiO_2$. Although the TBA-$TiO_2$-derived films are thinner than Com-$TiO_2$-derived films (8 $\mu$m vs 11 $\mu$m), the absorbance of N719-dye on TBA-$TiO_2$ type films was found to be 1.42 times greater than by the same dye on Com-$TiO_2$ type films, when measured at the dye spectral maximum (537 nm; Figure 3A). Following dye loading, TBA-$TiO_2$-derived films are visibly darker than Com-$TiO_2$-derived films. To facilitate absolute comparisons of the amount of dye adsorbed by each type of material, we divided the measured UV−vis absorption spectra by the thicknesses of the corresponding films (see SI). The thickness-normalized absorbance of N719 on TBA-$TiO_2$-derived films was found to be 1.9 times greater than on Com-$TiO_2$-derived films. This value is in good agreement with the ratio (1.8) of volume-normalized (thickness-normalized) surface areas ($A_V$).

With these differences in dye-loading in mind, we compared the performance of TBA-$TiO_2$- and Com-$TiO_2$-derived films in N719-containing DSSCs. (Prior to dye loading and cell incorporation, both types of films were coated with a light-scattering layer of $TiO_2$ particles of ~400 nm diameter; see SI.) Plots of photocurrent density ($J$) versus applied potential ($V$) were recorded for the cells at an intensity of 1 sun using simulated AM 1.5 light (Figure 3B). The Com-$TiO_2$-containing cell gave a short circuit photocurrent density ($J_{SC}$) of 12.0 mA $cm^{-2}$, an open circuit voltage ($V_{OC}$) of 724 mV, a fill factor (FF) of 0.75, and an overall light-to-electrical-energy conversion efficiency ($\eta$) of 6.6%. The same measurement with a TBA-$TiO_2$-containing cell yielded substantially better performance: a $J_{SC}$ value of 17.7 mA $cm^{-2}$, a $V_{OC}$ of 767 mV, an FF of 0.71, and an overall efficiency of 9.6%.[18] The

(17) Barrett, E. P.; Joyner, L. G.; Halenda, P. P. *J. Am. Chem. Soc.* **1951**, *73*, 373–380.

(18) The *average* overall efficiency was 9.2%, with underperforming cells generally containing photoelectrodes having one or more visible cracks.

ratio of short-circuit photocurrent densities for the two types of cells (1.47:1; TBA-$TiO_2$:Com-$TiO_2$) is consistent with the ratio of dye absorbances (1.42). (More significantly, it is also consistent with the ratio of integrated light-harvesting efficiencies (1.38:1; TBA-$TiO_2$:Com-$TiO_2$).) These findings imply that the dye molecules are properly harvesting light, the TBA-$TiO_2$ NPs are well interconnected in the film, and the injected electrons are efficiently transported through the film to the current collector. Figure 3C shows incident photon-to-current conversion efficiencies (IPCEs) for the two types of cells in the range of 400−700 nm. In close agreement with the ratio of $J_{SC}$ values, the TBA-$TiO_2$-containing cell gives a 1.43-fold greater value for the integrated IPCE than does the Com-$TiO_2$-containing cell. Additionally, we found that the short-circuit photocurrent density of a representative TBA-$TiO_2$-containing cell correlated linearly with the intensity of the incident light over the range 0−170 mW $cm^{-2}$ (ca. 0 to 1.7 sun). This behavior shows that current flow in such cells is not limited by mass transport of the redox shuttle, even though the average pore-size of the photoelectrode material is much reduced in comparison to that of photoelectrodes constructed from commercial paste; see SI.

## Conclusions

In summary, small, amphiphilic $TiO_2$ NPs (~9 nm diameter) can be readily synthesized from TIP by using TBAOH. The particles can subsequently be used to prepare, with high reliability and in very few steps, α-terpineol-based $TiO_2$ pastes. These pastes are suitable for fabrication of highly transparent, mesoporous photoelectrodes. The electrodes are characterized by high, thickness-normalized, surface areas, ca. 1.4 times those obtained for electrodes fabricated from a standard, commercially available $TiO_2$ paste. Incorporation of the new electrodes into DSSCs reveals a ca. 1.4-fold improvement in overall energy conversion efficiency. While the observed value for $\eta$ for TBA-$TiO_2$-containing cells (9.6%) still falls short of the very highest efficiency values reported for DSSCs based on N719 ($\eta = 11+\%$),[8] we believe that the reported photoelectrode fabrication protocol will prove useful to researchers interested in constructing comparatively high efficiency cells in a simple, convenient, and reliable fashion.

**Acknowledgment.** This work was supported in part by the Argonne-Northwestern Solar Energy Research (ANSER) Center, an Energy Frontier Research Center funded by the U.S. Department of Energy, Office of Science, Office of Basic Energy Sciences, under Award Number DE-SC0001059. We also acknowledge the Korean Government for supporting N.C.J. through the program of the National Research Foundation of Korea, Grant NRF-2009-352-D00055. O.K.F. thanks the Northwestern NSEC for partial support.

**Supporting Information Available:** Experimental details, materials sources, photographs, TEM images, SEM images, XRD patterns, pore-size distributions, and BJH surface area calculations. This material is available free of charge via the Internet at http://pubs.acs.org.